Biotinylated dextran amine anterograde tracing of the canine corticospinal tract★

Xiao Han[1], Guangming Lv[1], Huiqun Wu[2], Dafeng Ji[1], Zhou Sun[1], Yaofu Li[1], Lemin Tang[3]

1Department of Human Anatomy, Institute of Neurobiology, Jiangsu Key Laboratory of Neuroregeneration, Medical School, Nantong University, Nantong 226001, Jiangsu Province, China
2Department of Medical Informatics, Institute of Digital Medicine, Medical School, Nantong University, Nantong 226001, Jiangsu Province, China
3Department of Medical Image Engineering, Medical School, Nantong University, Nantong 226001, Jiangsu Province, China

Abstract

In this study, biotinylated dextran amine (BDA) was microinjected into the left cortical motor area of the canine brain. Fluorescence microscopy results showed that a large amount of BDA-labeled pyramidal cells were visible in the left cortical motor area after injection. In the left medulla oblongata, the BDA-labeled corticospinal tract was evenly distributed, with green fluorescence that had a clear boundary with the surrounding tissue. The BDA-positive corticospinal tract entered into the right lateral funiculus of the spinal cord and descended into the posterior part of the right lateral funiculus, close to the posterior horn, from cervical to sacral segments. There was a small amount of green fluorescence in the sacral segment. The distribution of BDA labeling in the canine central nervous system was consistent with the course of the corticospinal tract. Fluorescence labeling for BDA gradually diminished with time after injection. Our findings indicate that the BDA anterograde tracing technique can be used to visualize the localization and trajectory of the corticospinal tract in the canine central nervous system.
Key Words: biotinylated dextran amine; corticospinal tract; anterograde tracing; fluorescence; canine
Abbreviations: CST, corticospinal tract; BDA, biotinylated dextran amine

Xiao Han★, Master, Lecturer, Department of Human Anatomy, Institute of Neurobiology, Jiangsu Key Laboratory of Neuroregeneration, Medical School, Nantong University, Nantong 226001, Jiangsu Province, China

Corresponding author: Guangming Lv, Ph.D., Professor, Department of Human Anatomy, Institute of Neurobiology, Jiangsu Key Laboratory of Neuroregeneration, Medical School, Nantong University, Nantong 226001, Jiangsu Province, China; Lemin Tang, Professor, Department of Medical Image Engineering, Medical School, Nantong University, Nantong 226001, Jiangsu Province, China
gmlu@ntu.edu.cn;
lemintang@ntu.edu.cn

INTRODUCTION

The corticospinal tract (CST) is a nerve tract that descends from the cerebral motor cortex and projects to anterior horn motor neurons of the spinal cord in mammals, mainly controlling voluntary skeletal muscle movements. Injury to the CST can cause loss of motor function. Previous studies on spinal cord injury indicate that the recovery of voluntary movement following spinal cord injury primarily depends on the regeneration of the CST[1-3]. Important morphological indices of CST regeneration are the anatomical localization of axon fibers and the reconstruction of neural circuitry. Therefore, the normal anatomical localization of the CST in the spinal cord is important for studies on CST regeneration and reconstruction following spinal cord injury.

Reproducible methods are required for monitoring the regrowth of CST processes to permit the evaluation of therapeutic strategies that stimulate CST regeneration. The commonly used myelin staining method is not able to accurately display the localization or structure of the CST in the white matter of the spinal cord[4-7]. Since the 1970s, horseradish peroxidase has been widely used for nerve tract tracing. However, there are some disadvantages, such as difficulty in determining proper injection site, long injection time, transneuronal transport and low sensitivity. Researchers have also used CST specific markers, such as protein kinase Cγ, for immunolocalization of the CST[8-9], but have failed to successfully use the method in dogs and human beings (unpublished data). In recent years, medical imaging techniques, such as diffusion tensor imaging, magnetic resonance tractography and transcranial magnetic stimulation, combined with computer three-dimensional reconstruction technology, have been used to study the morphological localization of the CST[10-13]. In addition, manganese-enhanced magnetic resonance imaging has been used to visualize the CST in living rats[14]. The neuronal tracer biotinylated dextran amine (BDA) is more frequently used in tracing experiments in rodents, such as rats and mice, than in large animals, such as dogs and cats[15-18]. These methods permit good localization of the CST in the brain, as well as in the cervical and superior thoracic segments of the spinal cord, but do not allow

proper visualization of the CST in the inferior spinal cord. Due to the fact that BDA-positive cells are mainly located in the CST below the medulla oblongata, this study aimed to anatomically localize the CST using BDA anterograde tracing of pyramidal cells in the canine cortical motor area (where the CST originates).

RESULTS

Quantitative analysis of experimental animals

A total of eight dogs were included in this study, and two animals each were selected for BDA anterograde tracing at 14, 28, 42 and 49 days after injection. All eight dogs were involved in the final analysis, with no loss.

BDA-labeled pyramidal cells in the canine cerebral cortex

A number of BDA-labeled pyramidal cells were stained green in the left motor area of the cerebral cortex where the BDA was injected (Figure 1). The positive cell bodies had a pyramidal shape, and the axons appeared as elongated stripes.
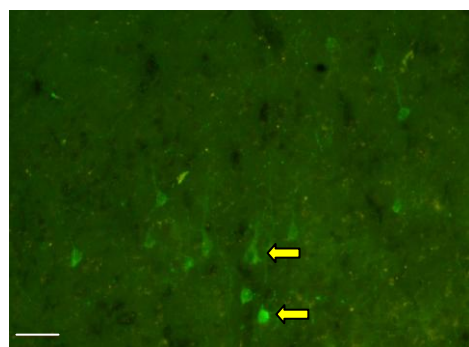

Figure 1   Biotinylated dextran amine fluorescence labeling of pyramidal cells in the canine motor cortex. Positive labeling is visible in green. Arrows indicate the bodies of pyramidal cells (scale bar: 100 μm).

BDA-labeled pyramidal cells in the canine medulla oblongata CST

BDA fluorescence labeling showed that the CST was distributed uniformly in the left pyramids of the medulla oblongata, while no positive staining was visible in the right hemisphere. The labeled CST was clearly distinguishable from the surrounding tissue and had a clear boundary (Figure 2). At the decussation in the lower part of the medulla oblongata, the green fluorescence-labeled axons traveled obliquely through the ventral midbrain aqueduct in the medulla oblongata and traversed across to the lateral funiculus of the contralateral spinal cord (Figure 3). The CST then descended along the posterior part of the lateral funiculus of the spinal cord near the posterior horn of the spinal gray matter in the cervical, thoracic, lumbar and sacral segments.
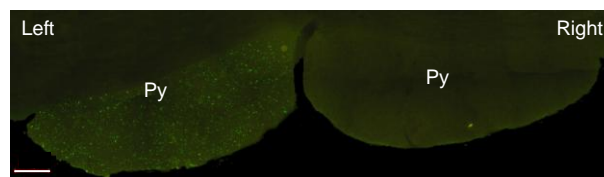

Figure 2   Biotinylated dextran amine fluorescence staining in the pyramid (Py) of the medulla oblongata (scale bar: 500 μm). Positive labeling is in green.
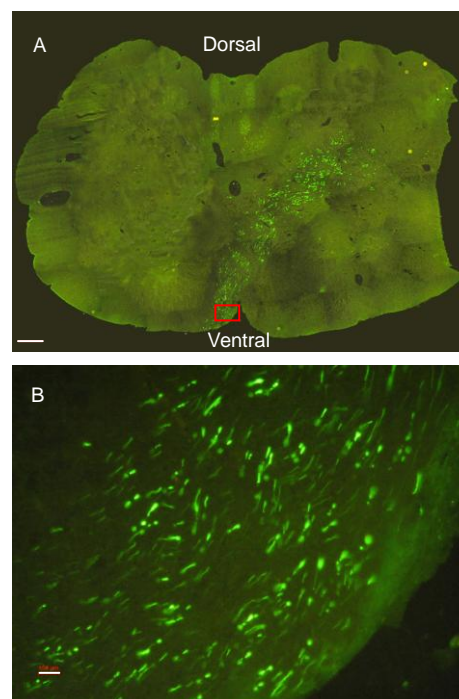

Figure 3   Biotinylated dextran amine fluorescence staining at the decussation of the pyramid. Positive labeling is in green.
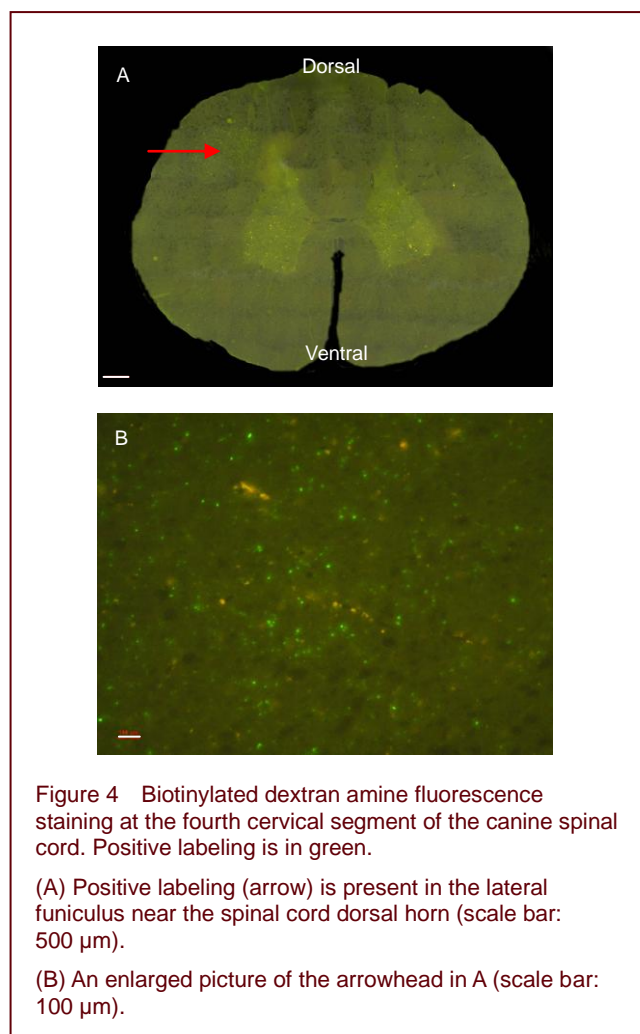
(A) Staining at the decussation of the pyramid of canines (scale bar: 500 μm).

(B) An enlarged picture (red rectangle shown in A) of the green fluorescent area in A (scale bar: 100 μm).

Distribution and temporal profile of BDA labeling in the canine spinal cord

BDA fluorescence staining showed that the left lateral funiculus, the bilateral anterior funiculi and the posterior funiculi of the spinal cord were not labeled with BDA. In the right lateral funiculus of the spinal cord, the CST gradually shifted dorsally as it descended from cervical to sacral segments. At the fourth thoracic segment, the CST was located in the lateral funiculus near the spinal dorsal horn, while in the lumbar and sacral segments, the CST was less prominent than in the cervical and thoracic segments, and only several fluorescent fibers were observed in the sacral segments (Figure 4). The distribution of BDA labeling in the central nervous system

of the dog was consistent with the trajectory of the CST. At 14 days after injection of BDA into the motor cortex, fluorescence labeling appeared in the motor cortex, the pyramids and the cervical spinal cord. No positive staining was visible below the thoracic segments. However, BDA labeling was visible in the eighth thoracic segment at 28 days and in sacral segments at 42 days. BDA labeling faded in all segments by 49 days, and no fluorescence was observed in the lumbar and sacral segments.

Figure 4   Biotinylated dextran amine fluorescence staining at the fourth cervical segment of the canine spinal cord. Positive labeling is in green.

(A) Positive labeling (arrow) is present in the lateral funiculus near the spinal cord dorsal horn (scale bar: 500 μm).

(B) An enlarged picture of the arrowhead in A (scale bar: 100 μm).

DISCUSSION

A number of studies have shown that the localization of the CST in the spinal cord varies significantly between different species of mammals. In rodents such as rats and mice, the CST travels across the pyramidal decussation and enters the contralateral posterior funiculus of the spinal cord, descending into lumbar and sacral segments[19-21]. In contrast, in the majority of carnivores and primates, the pathway taken by the CST is different. For example, in cats, dogs, monkeys, gorillas and humans, the CST travels through the pyramidal decussation to the dorsal side of the lateral funiculus of

the spinal cord, forming the lateral corticospinal tract which descends to sacral segments[22-23].

In the present study, an adapted BDA anterograde tracing method[24-25] was employed to observe CST localization in the central nervous system. The path of the CST determined by this method was consistent with previous reports. To avoid the limitations of classical histochemical staining using diaminobenzidine, streptavidin-fluorescein isothiocyanate[26-27] was used to visualize biotin-conjugated BDA, and the positive signal was easily observed under the fluorescence microscope at 488 nm excitation. In this study, the BDA-labeled CST was visible as a green fluorescent belt, uniformly and intensely distributed in the pyramid on the ventral aspect of the medulla oblongata in the injected side. No positive staining was present in the contralateral side. It was also observed that, at the pyramidal decussation at the lower end of the medulla oblongata, the labeled axons traveled through the ventral aspect of the central canal of the medulla oblongata, crossed over to the contralateral side and entered the lateral funiculus. The labeled fibers then descended close to the posterior horn of the spinal gray matter *via* the posterior part of the lateral funiculus in the cervical, thoracic, lumbar and sacral segments. No staining was observed in the bilateral anterior funiculi or the posterior funiculi. This fluorescence labeling method is simpler than immunohistochemical staining, and can exhibit a sharp border around the positive area. In our case, the labeling was easy to observe, and we obtained satisfactory results. Compared with other neural tracing methods, such as florescence red or gold, or virus-mediated tracing, the BDA labeling method is more convenient and provides satisfactory results.

After BDA absorption, time is required for the pyramidal neurons to transport the BDA to the distal part of the axons. Therefore, it is necessary to investigate the time required for BDA transport from the cerebral cortex to each spinal segment. This study revealed that at 14 days after BDA injection into the motor cortex, fluorescence was visible in the motor cortex, pyramids and cervical spinal cord, while no staining was visible below the thoracic segments. BDA labeling descended to the eighth thoracic segment at 28 days and to the sacral segments at 42 days. BDA fluorescence was not obvious in any segment at 49 days, and no positive staining was present in lumbar and sacral segments. This may be associated with CST length, speed of axonal transport, and influence of metabolic factors[28-29]. Therefore, to accurately evaluate BDA tracing of nerve fiber bundles, factors such as injection method, BDA dosage and concentration, and experimental procedure for label detection should be taken into consideration.

In summary, the BDA anterograde fluorescence tracing method is not only able to clearly display location, pathway, morphology and fiber connectivity, but also can be applied to studies addressing CST injury and regeneration. The ability of BDA-labeled nerve fibers to grow through the injured region is used to judge nerve

fiber regeneration and the reconstruction of nerve fiber circuitry[30-32]. Thus, the BDA fluorescence tracing technique is suitable for studies of CST anatomy, fiber connectivity, physiological function, and nerve injury and repair.

MATERIALS AND METHODS

Design
An animal study.
Time and setting
The experiment was performed at the Department of Human Anatomy, Institute of Neurobiology, Jiangsu Key Laboratory of Neuroregeneration, Medical School, Nantong University, China, from May 2009 to September 2010.
Materials
A total of eight healthy adult mongrel dogs, aged 4 years, clean grade, weighing 4.8−5.2 kg, three males and five females, were provided by the Laboratory Animal Center of Nantong University, China (license No. SYXK (Su) 2007-0021). All animals were kept in an environment with a 12-hour light/dark cycle, allowing free access to food and water. All animal experiments were conducted according to protocols approved by the United States National Institutes of Health Guide for the Care and Use of Laboratory Animals.
Methods
BDA anterograde tracing
Each canine was anesthetized with an intraperitoneal injection of 3% sodium pentobarbital (1 mL/kg) and then mounted with a stereotaxic device (Kiangwan, Shanghai, China). A piece of skull of 10 mm diameter was cut off by skull perforation (AI Biological Research, Shanghai, China) to expose the left cortical motor area[33-34]. 10% BDA (10 000 molecular weight; N-7167, Molecular Probes, Carlsbad, CA, USA)[35] solution was slowly injected into the cerebral motor cortex at 24 sites to a depth of 2.5 mm. Each site received 0.5 µL BDA solution. After injection, the brain surface was covered with a thin sterile absorbable gelatin sponge, and the scalp was sutured. At 14, 28, 42 and 49 days after injection, two canines each were anesthetized by intraperitoneal injection of the compound anesthetic Chlorpent (0.2 mL/100 g) and perfused transcardially for 1 hour with 0.9% saline (4°C) and then 4% phosphate-buffered paraformaldehyde (pH 7.4). Subsequently, the whole brain and spinal cord were dissected, fixed for 24 hours and paraffin embedded. 30 µm-thick coronal sections were prepared using a Leica cryostat (Leica, Wetzlar, Germany). All the sections were kept at 4°C until use.
BDA fluorescence staining
Sections were rinsed in 0.01 M phosphate-buffered saline, incubated in streptavidin-fluorescein isothiocyanate (1:500; Invitrogen, Carlsbad, CA, USA; code No: 43-4311, diluted with 0.01 M phosphate-buffered saline containing 0.3% Triton X-100) for 24 hours at room temperature. After rinsing with 0.01 M

phosphate-buffered saline, sections were mounted and observed under a Leica DMR fluorescence microscope (Leica, Wetzlar, Germany) with excitation at 488 nm.
Image acquisition and processing
Because of the limitations of the fluorescence microscope, images of each section were acquired under a 10 × objective lens with Leica Qwin image processing software (Leica) and spliced into a complete image to provide accurate CST localization in the brain and spinal cord. All images were obtained with the same imaging conditions, and saved as JPG files with a resolution of 2 272 × 1 704 pixels.

REFERENCES

[1]   Krassioukov A. Autonomic function following cervical spinal cord injury. Respir Physiol Neurobiol. 2009;169(2):157-164.
[2]   Fawcett J. Repair of spinal cord injuries: where are we, where are we going? Spinal Cord. 2002;40(12):615-623.
[3]   Vinit S, Kastner A. Descending bulbospinal pathways and recovery of respiratory motor function following spinal cord injury. Respir Physiol Neurobiol. 2009;169(2):115-122.
[4]   Joosten EA. Corticospinal tract regrowth. Prog Neurobiol. 1997; 53(1):1-25.
[5]   Tóth IE, Banczerowski P, Boldogkoi Z, et al. Cerebral neurons involved in the innervation of both the adrenal gland and the ovary: a double viral tracing study. Brain Res Bull. 2008;77(5):306-311.
[6]   Liang H, Paxinos G, Watson C. Projections from the brain to the spinal cord in the mouse. Brain Struct Funct. 2011;215(3-4): 159-186.
[7]   Lanciego JL, Wouterlood FG. A half century of experimental neu-roanatomical tracing. J Chem Neuroanat. 2011;42(3): 157-183.
[8]   Hughes AS, Averill S, King VR, et al. Neurochemical characterization of neuronal populations expressing protein kinase C gamma isoform in the spinal cord and gracile nucleus of the rat. Neuroscience. 2008;153(2):507-517.
[9]   Higo N, Oishi T, Yamashita A, et al. Expression of protein kinase-C substrate mRNA in the motor cortex of adult and infant macaque monkeys. Brain Res. 2007;1171:30-41.
[10]   Siebner HR, Rothwell J. Transcranial magnetic stimulation: new insights into representational cortical plasticity. Exp Brain Res. 2003;148(1):1-16.
[11]   Imfeld A, Oechslin MS, Meyer M, et al. White matter plasticity in the corticospinal tract of musicians: a diffusion tensor imaging study. Neuroimage. 2009;46(3):600-607.
[12]   Kovanlikaya I, Firat Z, Kovanlikaya A, et al. Assessment of the corticospinal tract alterations before and after resection of brainstem lesions using Diffusion Tensor Imaging (DTI) and tractography at 3T. Eur J Radiol. 2011;77(3):383-391.

[13] Matsuda K, Wang HX, Suo C, et al. Retrograde axonal tracing using manganese enhanced magnetic resonance imaging. Neuroimage. 2010;50(2):366-374.

[14] Luppi PH, Fort P, Jouvet M. Iontophoretic application of unconjugated cholera toxin B subunit (CTb) combined with immunohistochemistry of neurochemical substances: a method for transmitter identification of retrogradely labeled neurons. Brain Res. 1990;534(1-2):209-224.

[15] Wouterlood FG, Vinkenoog M, van den Oever M. Tracing tools to resolve neural circuits. Network. 2002;13(3):327-342.

[16] Griffin JW, Pan B, Polley MA, et al. Measuring nerve regeneration in the mouse. Exp Neurol. 2010;223(1):60-71.

[17] Leite-Almeida H, Almeida A. Novel applications of common stereology software to represent the complete distribution, density and spatial organization of anterogradely labelled fibers in neuroanatomical tract-tracing studies. J Neurosci Methods. 2007; 163(1):17-23.

[18] Steward O, Zheng B, Tessier-Lavigne M, et al. Regenerative growth of corticospinal tract axons via the ventral column after spinal cord injury in mice. J Neurosci. 2008;28(27):6836-6847.

[19] Canty AJ, Murphy M. Molecular mechanisms of axon guidance in the developing corticospinal tract. Prog Neurobiol. 2008;85(2): 214-235.

[20] Steward O, Zheng B, Ho C, et al. The dorsolateral corticospinal tract in mice: an alternative route for corticospinal input to caudal segments following dorsal column lesions. J Comp Neurol. 2004; 472(4):463-477.

[21] Zhang Y, Xiong Y, Mahmood A, et al. Sprouting of corticospinal tract axons from the contralateral hemisphere into the denervated side of the spinal cord is associated with functional recovery in adult rat after traumatic brain injury and erythropoietin treatment. Brain Res. 2010;1353:249-257.

[22] Jeffery ND, Smith PM, Lakatos A, et al. Clinical canine spinal cord injury provides an opportunity to examine the issues in translating laboratory techniques into practical therapy. Spinal Cord. 2006; 44(10):584-593.

[23] Schieber MH. Chapter 2 Comparative anatomy and physiology of the corticospinal system. Handb Clin Neurol. 2007;82:15-37.

[24] Ferguson IA, Xian C, Barati E, et al. Comparison of wheat germ agglutinin-horseradish peroxidase and biotinylated dextran for anterograde tracing of corticospinal tract following spinal cord in-jury. J Neurosci Methods. 2001;109(2):81-89.

[25] Avens HJ, Bowman CN. Development of fluorescent polymerization-based signal amplification for sensitive and nonenzymatic biodetection in antibody microarrays. Acta Biomater. 2010;6(1):83-89.

[26] Pompolo S, Ischenko O, Pereira A, et al. Evidence that projections from the bed nucleus of the stria terminalis and from the lateral and medial regions of the preoptic area provide input to gonadotropin releasing hormone (GNRH) neurons in the female sheep brain. Neuroscience. 2005;132(2):421-436.

[27] Bowyer JF, Schmued LC. Fluoro-Ruby labeling prior to an amphetamine neurotoxic insult shows a definitive massive loss of dopaminergic terminals and axons in the caudateputamen. Brain Res. 2006;1075(1):236-239.

[28] Sozmen EG, Kolekar A, Havton LA, et al. A white matter stroke model in the mouse: axonal damage, progenitor responses and MRI correlates. J Neurosci Methods. 2009;180(2):261-272.

[29] Breuer AC, Bond M, Atkinson MB. Fast axonal transport is mod-ulated by altering trans-axolemmal calcium flux. Cell Calcium. 1992;13(4):249-262.

[30] Deumens R, Koopmans GC, Honig WM, et al. Limitations in transplantation of astroglia-biomatrix bridges to stimulate corti-cospinal axon regrowth across large spinal lesion gaps. Neurosci Lett. 2006;400(3):208-212.

[31] Steward O, Zheng B, Tessier-Lavigne M, et al. Regenerative growth of corticospinal tract axons via the ventral column after spinal cord injury in mice. J Neurosci. 2008;28(27):6836-6847.

[32] Anderson KD, Sharp KG, Steward O. Bilateral cervical contusion spinal cord injury in rats. Exp Neurol. 2009;220(1):9-22.

[33] Tanaka D Jr. Differential laminar distribution of corticostriatal neurons in the prefrontal and pericruciate gyri of the dog. J Neurosci. 1987;7(12):4095-4106.

[34] Sakai ST, Stanton GB, Isaacson LG. Thalamic afferents of area 4 and 6 in the dog: a multiple retrograde fluorescent dye study. Anat Embryol (Berl). 1993;188(6):551-559.

[35] Li L, Gao XL, Song YZ, et al. Projections from cervical spinocerebellar tract neurons to cerebellar nuclei in rats by the anterograde labeling of biotinylated dextran amine. Zhongguo Linchuang Kangfu. 2006;10(46):129-131.

(Edited by Jin GH, He XJ//Yang Y/Song LP)